

# Decoherence in Attosecond Photoionization

Stefan Pabst,<sup>1,2</sup> Loren Greenman,<sup>3</sup> Phay J. Ho,<sup>4</sup> David A. Mazziotti,<sup>3</sup> and Robin Santra<sup>1,2,\*</sup>

<sup>1</sup>*Center for Free-Electron Laser Science, DESY, Notkestrasse 85, 22607 Hamburg, Germany*

<sup>2</sup>*Department of Physics, University of Hamburg, Jungiusstrasse 9, 20355 Hamburg, Germany*

<sup>3</sup>*Department of Chemistry and The James Franck Institute,  
The University of Chicago, Chicago, Illinois 60637, USA*

<sup>4</sup>*Argonne National Laboratory, Argonne, Illinois 60439, USA*

(Dated: February 16, 2022)

The creation of superpositions of hole states via single-photon ionization using attosecond extreme-ultraviolet pulses is studied with the *time-dependent configuration interaction singles* (TDCIS) method. Specifically, the degree of coherence between hole states in atomic xenon is investigated. We find that interchannel coupling not only affects the hole populations, it also enhances the entanglement between the photoelectron and the remaining ion, thereby reducing the coherence within the ion. As a consequence, even if the spectral bandwidth of the ionizing pulse exceeds the energy splittings among the hole states involved, perfectly coherent hole wave packets cannot be formed. For sufficiently large spectral bandwidth, the coherence can only be increased by increasing the mean photon energy.

PACS numbers: 32.80.Aa, 42.65.Re, 03.65.Yz

The typical time scale of electronic motion in atoms, molecules, and condensed matter systems ranges from a few attoseconds ( $1 \text{ as} = 10^{-18} \text{ s}$ ) to tens of femtoseconds ( $1 \text{ fs} = 10^{-15} \text{ s}$ ) [1–3]. In the last decade the remarkable progress in high harmonic generation [4–8] made it possible to generate attosecond pulses as short as 80 as [9]. Attosecond pulses have opened the door to real-time observations of the most fundamental processes on the atomic scale [1, 10]. For instance, the generation of attosecond pulses was utilized to determine spatial structures of molecular orbitals [11]; an interferometric technique using attosecond pulses was used to characterize attosecond electron wave packets [12]; and attosecond pulse trains [13] and isolated attosecond pulses [14], in combination with an intense few-cycle infrared pulse, enabled the control of electron localization in molecules. Attosecond technology demonstrated the ability to follow, on a subfemtosecond time scale, processes such as photoionization [15], Auger decay [16], and valence electron motion driven by relativistic spin-orbit coupling [17]. Furthermore, the availability of attosecond pulses fuelled a broad interest in exploring charge transfer dynamics following photoexcitation or photoionization [14].

In this Letter, we analyze the creation of hole states via single-photon ionization using a single extreme-ultraviolet attosecond pulse. We investigate the impact of the freed photoelectron on the remaining ion and demonstrate that the interaction between the photoelectron and the ion cannot be neglected for currently available state-of-the-art attosecond pulses. In particular, the interchannel coupling of the initially coherently excited hole states greatly enhances the entanglement between the photoelectron and the ionic states. Interchannel coupling is mediated by the photoelectron and mixes different ionization channels, i.e., hole configurations, with

each other. Consequently, the degree of coherence among the ionic states is strongly reduced, making it impossible to describe the subsequent charge transfer in the ion with a pure quantum mechanical state. Experiments on photosynthetic systems [18–21] have revealed a correlation between highly efficient energy transport and coherent dynamics in molecules (nuclear and electronic dynamics in this case). Similarly, high degrees of coherence in nonstationary hole states may be necessary for efficient charge transport within molecules.

In the last decade, much work has been done in the realm of hole migration [22–24]. It was shown that electronic motion can be triggered solely by electron correlation [22]. Charge transfers mediated by electronic correlations typically take place in a few femtoseconds and are thus faster than electronic dynamics initiated by nuclear motion [25, 26]. Recent experiments [27, 28] have demonstrated that electronically excited ionic states can modify site-selective reactivity within tens of femtoseconds, making hole migration processes a promising tool to control chemical reactions. Up to now, theoretical calculations [22, 24] investigating hole migration phenomena have neglected the interaction between the parent ion and the photoelectron and assumed a perfectly coherent hole wave packet. As long as the photoelectron departs sufficiently rapidly from the parent ion, this assumption is appropriate [29]. However, for attosecond pulses with large spectral bandwidths, the enhanced production of slow photoelectrons will affect (mainly via interchannel coupling) both the final hole populations and the coherence among these hole states. Furthermore, recent results in high harmonic spectroscopy suggest that interchannel coupling may be the missing link to understand hole dynamics occurring in high harmonic generation processes before the ejected electron recombines with the parent

ion [30].

We investigate the creation of hole states via attosecond photoionization using the implementation of the time-dependent configuration-interaction singles (TDCIS) approach described in Ref. [31] (see also [32, 33]). TDCIS allows us to study ionization dynamics beyond the single-channel approximation and to understand systematically the relevance of interchannel coupling in the hole creation process. The TDCIS wave function for the entire system is

$$|\Psi(t)\rangle = \alpha_0(t) |\Phi_0\rangle + \sum_{a,i} \alpha_i^a(t) |\Phi_i^a\rangle, \quad (1)$$

where  $|\Phi_0\rangle$  is the Hartree-Fock ground state and  $|\Phi_i^a\rangle = \hat{c}_a^\dagger \hat{c}_i |\Phi_0\rangle$  is a one-particle-one-hole excitation ( $\hat{c}_a^\dagger$  and  $\hat{c}_i$  are creation and annihilation operators for an electron in orbitals  $a$  and  $i$ , respectively). The corresponding coefficients  $\alpha_0(t)$  and  $\alpha_i^a(t)$ , respectively, are functions of time and describe the dynamics of the system. Throughout, indices  $i, j$ , are used for occupied orbitals in  $|\Phi_0\rangle$ ; indices  $a, b$ , stand for unoccupied orbitals. We focus our discussion on the case where single-photon ionization is the dominant effect and higher order processes can be neglected. Our model system is atomic xenon. The corresponding Hamiltonian (neglecting spin-orbit coupling) is

$$\hat{H}(t) = \hat{H}_0 + \hat{H}_1 + E(t) \hat{z}, \quad (2a)$$

where  $E(t)$  is the electric field,  $\hat{z}$  the dipole operator, and  $\hat{H}_0$  is the mean-field Fock operator, which is diagonal with respect to the basis used in Eq. (1). The residual Coulomb interaction,

$$\hat{H}_1 = \hat{V}_c - \hat{V}_{\text{MF}}, \quad (2b)$$

is defined such that  $\hat{H}_0 + \hat{H}_1$  gives the exact nonrelativistic Hamiltonian for the electronic system in the absence of external fields ( $\hat{V}_c$  is the electron-electron interaction). We study the impact of different approximations for  $\hat{H}_1$  on the hole state as follows. The *Coulomb-free* model, the simplest approximation, removes the residual Coulomb interaction ( $\hat{H}_1 = 0$ ) between the excited electron and the parent ion. In this approximation, the excited electron always sees a neutral atom via the  $\hat{V}_{\text{MF}}$  potential [34]. A more realistic approximation is the *intrachannel* model including direct and exchange contributions of the Coulomb interaction only within a given channel. In this second model, the excited electron can only interact with the occupied orbital from which it originates. Interactions between different occupied orbitals are neglected, i.e. we set  $\langle \Phi_i^a | \hat{H}_1 | \Phi_j^b \rangle = 0$  for  $i \neq j$ . The third and final model describes the Coulomb interaction exactly within the TDCIS framework. We refer to this as the *full* model. Note that the exact nonrelativistic Hamiltonian  $\hat{H}_0 + \hat{H}_1$  is diagonal with respect to the

ionic one-hole states  $|\Phi_i\rangle = \hat{c}_i |\Phi_0\rangle$ . In the full model, the photoelectron can couple the hole states, as  $\hat{H}_1$  in the particle-hole space is not diagonal with respect to the hole index (i.e.,  $\langle \Phi_i^a | \hat{H}_1 | \Phi_j^b \rangle$  generally differs from zero). This type of photoelectron-mediated interaction is called interchannel coupling [35]. As a consequence, in the full model the hole index is not a good quantum number, whereas in the Coulomb-free and intrachannel models, excited eigenstates of  $\hat{H}_0 + \hat{H}_1$  are characterized by a well-defined hole index. To describe the hole states of the remaining ion, we employ the ion density matrix [31]

$$\hat{\rho}_{i,j}^{\text{IDM}}(t) = \text{Tr}_a[|\Psi(t)\rangle \langle \Psi(t)|]_{i,j} = \sum_a \langle \Phi_i^a | \Psi(t) \rangle \langle \Psi(t) | \Phi_j^a \rangle$$

where  $\text{Tr}_a$  stands for the trace over the photoelectron. The properties of the ion density matrix can be measured using attosecond transient absorption spectroscopy [17]. A description of the cationic eigenstates in terms of one-hole configurations is a physically meaningful approximation for noble-gas atoms such as xenon [36].

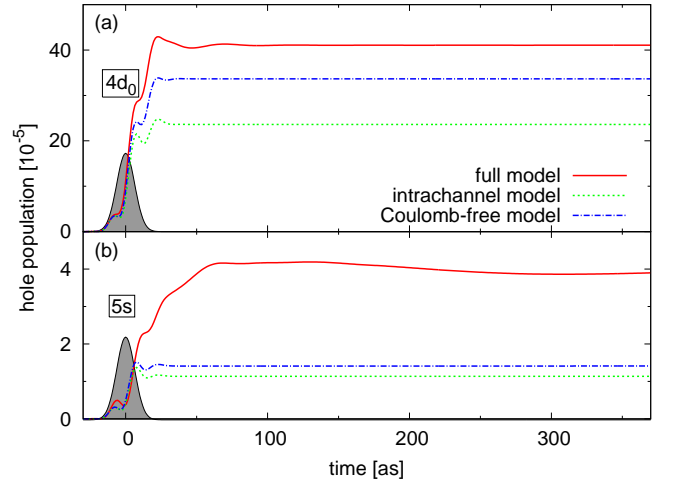


FIG. 1: (color online) The  $4d_0$  [panel (a)] and  $5s$  [panel (b)] hole populations of xenon as a function of time are shown for three different residual Coulomb interaction approximations: (1) the full model (red solid line), (2) the intrachannel model (green dotted line), and (3) the Coulomb-free model (blue dash-dotted line). The attosecond pulse has a peak field strength of 25 GV/m, a pulse duration of 20 as, a (mean) photon energy of 136 eV, and is centered at  $t = 0$  as.

In Fig. 1 the hole populations  $\rho_{5s,5s}^{\text{IDM}}(t)$  and  $\rho_{4d_0,4d_0}^{\text{IDM}}(t)$  of the xenon  $5s$  and  $4d_0$  orbitals, respectively, are shown for all three interaction models ( $4d_0$  stands for the  $4d$  orbital with  $m = 0$ ). The ionizing, gaussian-shaped attosecond pulse is linearly polarized and has a peak field strength of 25 GV/m, a pulse duration of  $\tau = 20$  as, and a (mean) photon energy of  $\omega_0 = 136$  eV. The hole dynamics of the Coulomb-free and intrachannel models

are alike. In both cases, the population is constant after the pulse, since the hole index is a good quantum number within these models. The extension to the exact Coulomb interaction changes the situation. Interchannel coupling causes the hole populations to remain nonstationary as long as the photoelectron remains close to the ion. As the distance between the photoelectron and the ion increases, the interchannel coupling weakens and the populations  $\rho_{i,i}^{\text{IDM}}(t)$  become stationary (see Fig. 1). We confine our discussion to the first hundreds of attoseconds after the pulse, allowing us to neglect decay processes, which start to take place after a few femtoseconds.

As we will see in the following, interchannel coupling not only affects the hole populations but also the coherence between the created hole states. The degree of coherence between  $|\Phi_i\rangle$  and  $|\Phi_j\rangle$  is given by

$$g_{i,j}(t) = \frac{|\rho_{i,j}^{\text{IDM}}(t)|}{\sqrt{\rho_{i,i}^{\text{IDM}}(t)\rho_{j,j}^{\text{IDM}}(t)}}. \quad (4)$$

Totally incoherent statistical mixtures result in  $g_{i,j}(t) = 0$ . The fact that the density matrix is positive semidefinite implies the Cauchy-Schwarz relations  $|\rho_{i,j}^{\text{IDM}}(t)|^2 \leq \rho_{i,i}^{\text{IDM}}(t)\rho_{j,j}^{\text{IDM}}(t)$ , which bound the maximum achievable (perfect) coherence ( $g_{i,j}(t) = 1$ ). To investigate the effect of interchannel coupling on the coherence between the orbitals  $4d_0$  and  $5s$  in xenon, we restrict the definition of the  $4d_0$  hole population to the events where the photoelectron has angular momentum  $l = 1$ . The other possible angular momentum for the  $4d_0$  photoelectron,  $l = 3$ , does not contribute to the coherence, since the photoelectron from  $5s$  can only have  $l = 1$ . For a similar reason, it is impossible to create a coherent superposition of  $5p$  and  $5s$  (or  $4d$ ) hole states via one-photon absorption in the electric dipole approximation.

Figure 2 illustrates the time evolution of the coherence between  $4d_0$  and  $5s$  in xenon for different pulse durations and fixed photon energy ( $\omega_0 = 136$  eV). Here, we use the full interaction model. Directly after the ionizing pulse is over, the initial degree of coherence (at  $t \approx 0$  as) rises with decreasing pulse duration, i.e., increasing spectral bandwidth, and converges to a value close to unity. (The difference of the ionization potentials,  $\varepsilon_{5s} - \varepsilon_{4d_0}$ , is  $\approx 50$  eV.) At  $t \approx 0$  as, the photoelectron is still in immediate contact with the parent ion. Therefore, the coherence properties of the system of interest—the parent ion—are affected by its interaction with the bath represented by the photoelectron. The system–bath interaction leads to a reduction in the coherence of the system [37], which can be seen by the rapid drops in all curves in Fig. 2 within tens of attoseconds after the pulse. With time, as the photoelectron departs from the ion, the Coulomb (“system–bath”) interaction becomes less important and the coherence converges to a stationary value. The maximum for this stationary value is obtained with a 25 as pulse ( $g_{4d_0,5s} \approx 0.6$ ). For pulses

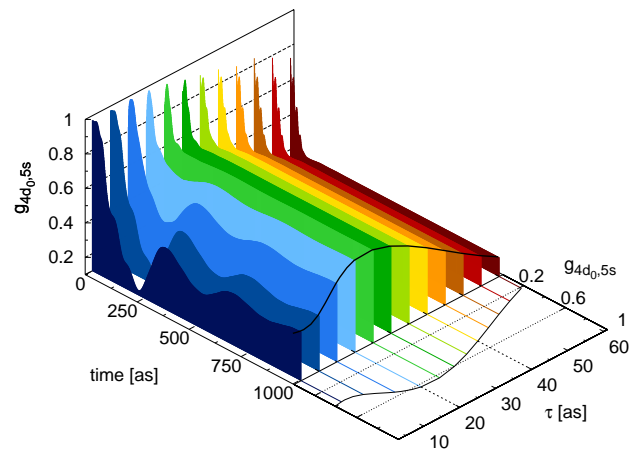


FIG. 2: (color online) The time evolution of the coherence between the  $4d_0$  and  $5s$  hole states in xenon is shown for the full Coulomb interaction model. The photon energy is 136 eV and the pulse duration varies from 5–60 as.

shorter than 25 as, oscillations in  $g_{4d_0,5s}$  occur that persist for hundreds of attoseconds, and the final degree of coherence reached falls below 0.6. The spin-orbit dynamics associated with the fine-structure within the  $4d$  shell is slow in comparison to the time scale of the decoherence between  $4d_0$  and  $5s$ , and is, therefore, not considered here.

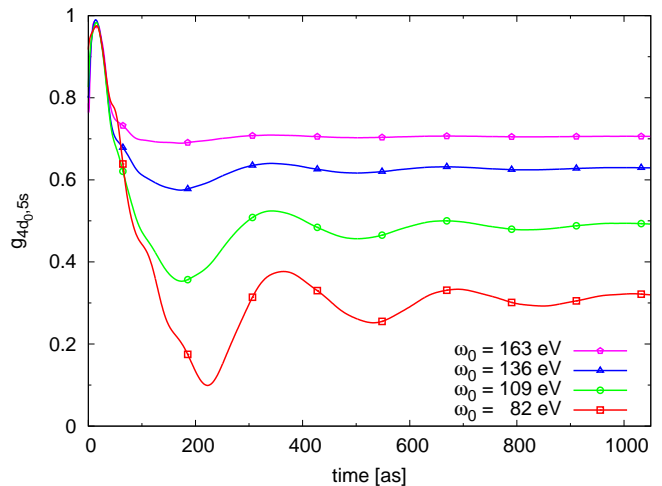


FIG. 3: (color online) The time evolution of the coherence between the  $4d_0$  and  $5s$  hole states, calculated with the full Coulomb interaction model, is shown for different photon energies. The pulse duration is in all cases 20 as.

We see in Fig. 3 that when holding the pulse duration fixed ( $\tau = 20$  as), the degree of coherence rises with increasing  $\omega_0$ . The magnitude of the oscillations decreases as the final coherence (at  $t \approx 1$  fs) increases. This trend indicates less system–bath interactions occur with higher

photoelectron energies keeping the degree of coherence among the hole states high.

In Fig. 4 we compare the impact of the different Coulomb approximations on the final coherence. The drops in coherence that occur for the full model for short pulses [Fig. 4(a)] and low photon energies [Fig. 4(b)] cannot be seen in the Coulomb-free and intrachannel models—which both neglect interchannel coupling. Hence, the decay of coherence is solely driven by the interchannel coupling due to the slow photoelectron. As a comparison to the Coulomb-free model shows, intrachannel coupling affects the coherence in an insignificant way. In the limit of long pulse durations (small spectral

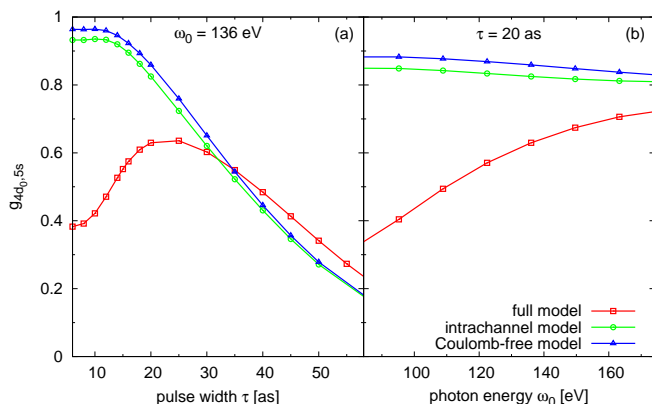


FIG. 4: (color online) The dependence of the coherence between the  $4d_0$  and  $5s$  hole states as function of the pulse duration (a) and as function of the photon energy (b) are shown for all three interaction approximations.

bandwidths), the coherence vanishes for all models, since photoelectrons from the  $4d_0$  and  $5s$  become energetically distinguishable and cannot contribute to a coherent statistical mixture of hole states. The slight drop in the coherence for the Coulomb-free and intrachannel models with increasing  $\omega_0$  [Fig. 4(b)] is related to the reduced factorizability of the numerator of Eq. (4). In contrast, the trend in the full model for increasing  $\omega_0$  is dominated by the gain in coherence due to higher photoelectron energy resulting in less system-bath interaction.

In conclusion, we demonstrated that the coherence of the ionic states produced via attosecond photoionization is not solely determined by the bandwidth of the ionizing pulse, but greatly depends on the kinetic energy of the photoelectron, which can be controlled by the (mean) photon energy. Interchannel coupling leads to an enhanced entanglement between the photoelectron and the parent ion resulting in a reduced coherence in the ionic states. This reduction can be mitigated with higher photon energies, thereby sacrificing high photon cross sections and the possibility of controlling independently the relative populations of the various hole states in the statistical mixture.

Our results have far-reaching consequences beyond the atomic case. Molecules will be even more strongly affected by interchannel coupling due to the reduced symmetry and smaller energy splittings between the cation many-electron eigenstates. Interchannel coupling is also likely to be significant for inner-valence hole configurations in molecules, which show strong mixing to configurations outside the TDCIS model space. The present study suggests that interchannel coupling accompanying the hole creation process will affect attosecond experiments investigating charge transfer processes in photoionized systems. The control of decoherence requires widely tunable attosecond sources, thus offering a new opportunity for x-ray free-electron lasers [38].

P.J.H. was supported by the Office of Basic Energy Sciences, U.S. Department of Energy under Contract No. DE-AC02-06CH11357. L.G. thanks Martha Ann and Joseph A. Chenicek and their family. D.A.M. gratefully acknowledges the NSF, the Henry-Camille Dreyfus Foundation, the David-Lucile Packard Foundation, and the Microsoft Corporation for their support.

\* Corresponding author; Electronic address: robin.santra@cfel.de

- [1] F. Krausz and M. Ivanov, Rev. Mod. Phys. **81**, 163 (2009).
- [2] A. H. Zewail, J. Phys. Chem. A **104**, 5660 (2000).
- [3] A. L. Cavalieri *et al.*, Nature **449**, 1029 (2007).
- [4] G. Doumy *et al.*, Phys. Rev. Lett. **102**, 093002 (2009).
- [5] N. Dudovich *et al.*, Nature Phys. **2**, 781 (2006).
- [6] R. López-Martens *et al.*, Phys. Rev. Lett. **94**, 033001 (2005).
- [7] E. A. Gibson *et al.*, Phys. Rev. Lett. **92**, 033001 (2004).
- [8] K. J. Schafer *et al.*, Phys. Rev. Lett. **70**, 1599 (1993).
- [9] E. Goulielmakis *et al.*, Science **320**, 1614 (2008).
- [10] T. Pfeifer *et al.*, Chem. Phys. Lett. **463**, 11 (2008).
- [11] S. Haessler *et al.*, Nature Phys. **6**, 200 (2010).
- [12] J. Mauritsson *et al.*, Phys. Rev. Lett. **105**, 053001 (2010).
- [13] K. P. Singh *et al.*, Phys. Rev. Lett. **104**, 023001 (2010).
- [14] G. Sansone *et al.*, Nature **465**, 763 (2010).
- [15] E. Skantzakis *et al.*, Phys. Rev. Lett. **105**, 043902 (2010).
- [16] M. Drescher *et al.*, Nature **419**, 803 (2002).
- [17] E. Goulielmakis *et al.*, Nature **466**, 739 (2010).
- [18] H. Lee, Y.-C. Cheng, and G. R. Fleming, Science **316**, 1462 (2007).
- [19] M. Sarovar *et al.*, Nature Phys. **6**, 462 (2010).
- [20] E. Collini *et al.*, Nature **463**, 644 (2010).
- [21] E. Harel, A. F. Fidler, and G. S. Engel, Proc. Natl. Acad. Sci. USA **107**, 16444 (2010).
- [22] J. Breidbach and L. S. Cederbaum, J. Chem. Phys. **118**, 3983 (2003).
- [23] M. Nest, F. Remacle, and R. D. Levine, New J. Phys. **10**, 025019 (2008).
- [24] A. Kuleff, S. Lünemann, and L. Cederbaum, J. Phys. Chem. A **114**, 8676 (2010).
- [25] D. Kröner *et al.*, Appl. Phys. A-Mater. **88**, 535 (2007).
- [26] B. H. Muskatel, F. Remacle, and R. D. Levine, Phys.

- Scripta **80**, 048101 (2009).
- [27] R. Weinkauf *et al.*, J. Phys. Chem. A **101**, 7702 (1997).
- [28] E. W. Schlag *et al.*, Angew. Chem. Int. Ed. **46**, 3196 (2007).
- [29] L. Cederbaum *et al.*, Adv. Chem. Phys. **65**, 115 (1986).
- [30] Y. Mairesse *et al.*, Phys. Rev. Lett. **104**, 213601 (2010).
- [31] L. Greenman *et al.*, Phys. Rev. A **82**, 023406 (2010).
- [32] H. B. Schlegel, S. M. Smith, and X. Li, J. Chem. Phys. **126**, 244110 (2007).
- [33] S. Klinkusch, P. Saalfrank, and T. Klamroth, J. Chem. Phys. **131**, 114304 (2009).
- [34] A. Szabo and N. S. Ostlund, *Modern Quantum Chemistry* (Dover, Mineola, NY, 1996).
- [35] A. F. Starace, Appl. Opt. **19**, 4051 (1980).
- [36] C. Buth, R. Santra, and L. S. Cederbaum, J. Chem. Phys. **119**, 7763 (2003).
- [37] H.-P. Breuer and F. Petruccione, *The Theory of Open Quantum Systems* (Oxford University Press, 2002).
- [38] A. Zholents and W. Fawley, Phys. Rev. Lett. **92**, 224801 (2004).